https://doi.org/10.5194/egusphere-2025-6366
Preprint. Discussion started: 11 February 2026

Evaluation of SWOT HR PIXC version D water level time series of small lakes

Simon Jakob Köhn[1] and Karina Nielsen[1]

[1]DTU Space, The Technical University of Denmark, Kongens Lyngby, Denmark

Correspondence: Simon Jakob Köhn (sijko@space.dtu.dk) and Karina Nielsen (karni@space.dtu.dk)

Abstract. Satellite altimetry has successfully monitored inland waters for more than 30 years and is increasingly important as the demand for freshwater grows and climate change accelerates. Launched in December 2022, the Surface Water and Ocean Topography (SWOT) satellite is the first to provide 2D spatially distributed elevation measurements, with a 21-day revisit time and better coverage depending on latitude and a nominal requirement to detect lakes as small as 0.06km^2. Here, we evaluate the SWOT L2 HR PIXC version D data product (if available at the time of writing) to construct time series of water surface elevation (WSE) and capture their relative WSE change in 37 Danish lakes with a surface area between 0.25km^2 and 40km^2 via the summary measures RMSE and Pearson's correlation coefficient (PCC). We tested six selection criteria to aggregate one WSE value per lake and timestamp. The median unbiased RMSE of SWOT vs gauge is 5.34cm, and the median PCC is 0.91. We find indications that SWOT's PIXC data contains time–varying residual roll–errors over Danish lakes. We demonstrate that our approach performs slightly better than filtered SWOT L2 HR LakeSP prior data from Hydrocron in terms of RMSE and PCC (6.05cm and 0.89), while retaining roughly double the number of valid timestamps over the overlapping period.

1 Introduction

Continental water resources are affected by climate and, therefore, are important markers of climate change. In addition, human activities continue to impact rivers and lakes, potentially devastating biodiversity and human existence (Best, 2019). Therefore, it is detrimental to continuously monitor the relative change in water surface elevation (WSE) of lakes and reservoirs worldwide to understand the underlying dynamics.

Traditionally, WSE is precisely measured by in–situ gauges, which can be expensive to install and maintain, and their data may not be public. In addition, the gauges are not evenly distributed across the Earth. Many lakes and rivers in remote areas and economically poor countries remain unobserved (Biancamaria et al., 2016). During the past 30 years, satellite altimetry has become an important, low-cost, freely available supplement in WSE monitoring (Abdalla et al., 2021). Globally distributed WSE time series are available from: Copernicus Land Monitoring Service (Copernicus, 2024), Hydroweb (Crétaux et al., 2011), "Database for Hydrological Time Series of Inland Waters (DAHITI)" (Schwatke et al., 2015), "USDA Lake database" (Birkett et al., 2011), and "ESA CCI Lake ECV" (Carrea et al., 2024; ESA, 2024).

The launch of the Surface Water and Ocean Topography (SWOT) satellite mission in December 2022, led by the Centre National d'Études Spatiales (CNES) and National Aeronautics and Space Administration (NASA), represents a new era in

https://doi.org/10.5194/egusphere-2025-6366
Preprint. Discussion started: 11 February 2026

satellite altimetry (Fu et al., 2024). It carries a dual–sided cross–track Ka–band Radar Interferometer (KaRIn) (JPL, 2024b), operating at 35.75GHz (Biancamaria et al., 2016), with near nadir incidence angles (Fjørtoft et al., 2014). The KaRIn instrument enables SWOT to sense WSE within two 50km wide swaths left and right of the satellite, separated by a 20km wide nadir gap (Biancamaria et al., 2016; JPL, 2024b). The highest available resolution data product, the High Rate (HR) PIXel Cloud (PIXC), retains measurements outside the defined swaths (JPL, 2023b). This makes SWOT the first altimetry satellite to observe 2D *images* of WSE. SWOT operates in a 21-day repeat science orbit (cycle) (JPL, 2024b) with an average global revisit time of 11 days (JPL, 2024a). The majority of all lakes are located above $50°$N (Lehner and Döll, 2004) which on average, will have at least 2-3 acquisitions per cycle (JPL/NASA, 2019; Biancamaria et al., 2016).

The unprecedented detail of SWOT data is expected to vastly improve our understanding of the dynamics of continental water bodies (Biancamaria et al., 2016) and by extent also of the Carbon (Cole et al., 1994) and Methane (Walter et al., 2007) budget. The dense spatial coverage enables studies of change at a regional scale, such as lake water storage, which is highly variable (Woolway et al., 2020). Importantly, with SWOT, the science objective is to monitor small lakes with an area down to 0.0625km^2 (JPL, 2024b) – which represent a significant fraction of global lakes (Taburet et al., 2020) – that previously were too small to be observed by nadir satellite altimetry missions effectively. SWOT certainly provides a more complete picture, enabling a better understanding and thus providing the basis for better decision–making.

Laipelt et al. (2025) and Simoes-Sousa et al. (2025) investigate the 2024 Brazil flood using the SWOT raster and the pixel cloud data, respectively, showing SWOT's potential for understanding floods and to estimate water volume. Buzzanga et al. (2025) perform a case study on Death Valley, finding SWOT to measure water with unprecedented detail that will improve our understanding of freshwater availability and management in the future. Yu et al. (2024) compares SWOT RiverSP and LakeSP water surface elevations against Hydroweb and G-REALM product data, finding a good agreement, and Wigneron et al. (2024) validates the 1–day (calibration/validation) orbit RiverSP data against other satellite altimeters for river WSE, confirming good preliminary results, and highlighting the unprecedented spatial resolution SWOT provides. Jacobs et al. (2025) show that residual systematic errors in the SWOT data are detectable relative to nadir satellite altimeters over the ocean, anticipated by Peral and Esteban-Fernandez (2018).

This study investigates the possibilities of constructing WSE time series from SWOT HR PIXC version D data and evaluates them against 37 gauged lakes with surface areas between 40 and 0.25km^2 and SWOT LakeSP prior time series as a baseline. Additionally, we find indications for a residual roll error in inland SWOT PIXC data on Danish lakes. Section 2 of this paper provides an overview of the data and study area, while Section 3 outlines the methods. Results are presented in Section 4 and discussed in Section 5. Lastly, we present our conclusion in Section 6.

2 Data and Study Area

2.1 SWOT

The joint CNES and NASA satellite SWOT was launched successfully on December 16, 2022. It carries a Ka-band radar interferometer as the main scientific instrument. The SWOT mission aims to enhance our understanding of the global water

https://doi.org/10.5194/egusphere-2025-6366
Preprint. Discussion started: 11 February 2026

cycle through measurements of ocean and inland surface water topography. It completed the initial calibration and test phase and has, since July 2023, been operating in its nominal 21-day science orbit (JPL, 2024b).

Inland water SWOT data is available in various products with different processing granularity. The most detailed information is available in the KaRIn water mask point cloud L2 HR PIXC data set (JPL, 2023b; SWOT, 2024b). Whereas the L2 HR LakeSP product (JPL, 2023a; SWOT, 2024a) assigns and aggregates the PIXC data to lakes from the "prior lake database" (PLD) (Wang et al., 2023). River data is analogously available in the L2 HR RiverSP product (SWOT, 2024c). Here, we primarily use the L2 HR PIXC data product version D as it provides the highest degree of freedom. From now on, we will refer to this dataset exclusively as PIXC. Initial investigations were done with the LakeSP product, but we found some issues for the small Danish lakes, where the WSE assignment to the PLD geometry resulted in assigning water to areas where no water is present. We have no reason to doubt the quality of the LakeSP product in other areas and expect it to improve over time.

We use all PIXC data within 57.2°–54.7°N and 8.1°–12.6°E. File duplicates are identified by the Composite Release Identifier (CRID) and product counter. Since the lakes included in the study have a sufficient number of "open water" observations, we only use class 4 PIXC data, and not "water near land" (class 3). At the time of writing, cycles 20 to 31 had not yet been reprocessed to version D. They are filled with process version C. Overall, SWOT PIXC data up to cycle 42, pass 458 (09.12.2025), were used.

We present prior LakeSP data from Hydrocron (Greguska et al., 2025) for comparison with our approach, using time series plots in the "Result" section. Currently, Hydrocron only provides process version C (until 02.05.2025 for Denmark), which we fully utilize. The LakeSP is filtered on $quality\_f = 0$, $xovr\_cal\_q = 0$ or 1, and $dark\_frac \leq 0.1$.

2.2 In–situ Gauges

In–situ stations measuring lake WSE are available through WSP (2024), combining multiple operator institutions. Most gauges cover the timeframe from the first SWOT 21–day science orbit cycle over Denmark (26.07.23) up to date. The gauge data has a daily resolution, and the water level is referenced to the Danish height system DVR90. To asses SWOT's ability to measure relative WSE change, we remove the median offset between SWOT and the gauge on a per–lake–basis, before reporting any metric. The offset for each gauge is listed in Table A1. The gauge uncertainty depends on the sensor. The water level is mainly measured with pressure and ultrasound sensors, where the uncertainty is listed as 15mm and 5mm-30mm (DMI, 2018).

2.3 Lake Geometries / Masks

The investigated lakes are exclusively located in Denmark and are selected from the 'sø' vector layer product of GeoDanmark (@geodanmark, 2024), documented in GeoDanmark (2018). The data set is updated cyclically every 5 years (KDS, 2024) and contains permanent lakes above $100 m^2$ in surface area. Additionally, the set of lakes used in this study is truncated below a surface area of $0.25 km^2$, leaving the 228 lakes, presented in Figure 1. The lake geometries are used to extract the relevant PIXC data. The available lake information from GeoDanmark is manually expanded by: annotating lake names, indicating whether a lake possesses a gauge, the gauge's IDs, location, and vertical reference. In total, 37 gauged lakes are used in the comparison. Their surface area distribution is shown in Figure A1D in the Appendix.

https://doi.org/10.5194/egusphere-2025-6366
Preprint. Discussion started: 11 February 2026

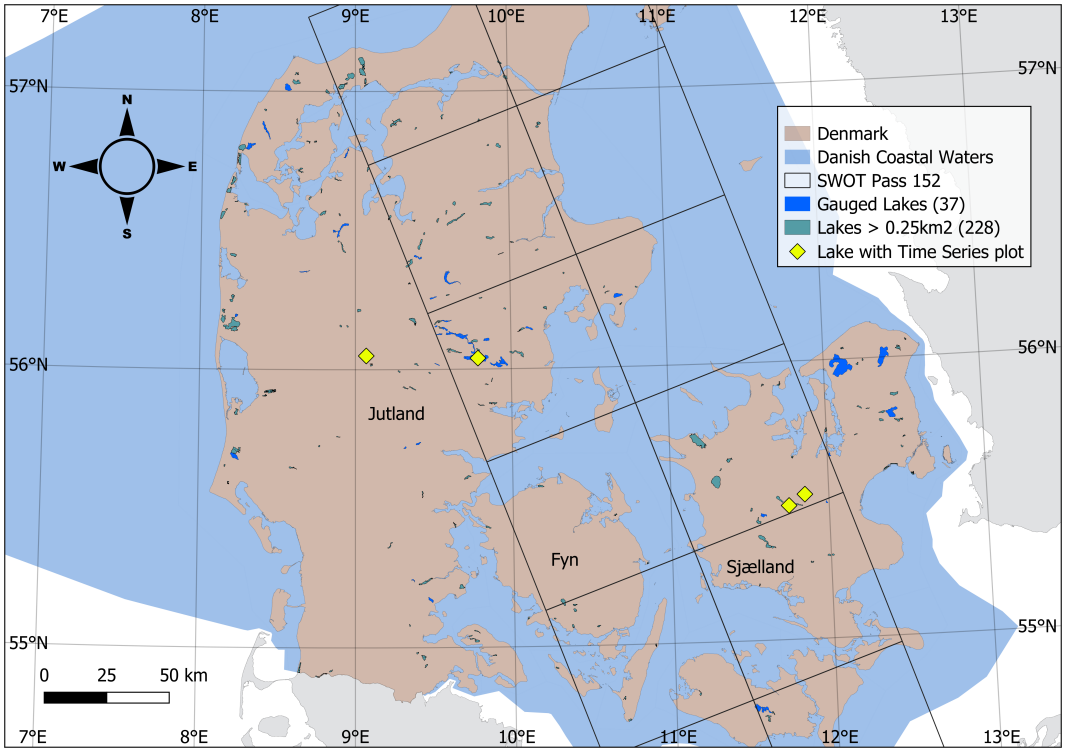

Figure 1. Map of Denmark with lakes larger than 0.25km^2. Detailed list of all gauged lakes is provided in Table A1. Danish shapefiles from @geodanmark (2024) and background borders from Sevdari and Marmullaku (2023).

3 Methods

3.1 Point Cloud Tile-Management and Masking

Lakes within one cycle and pass can be covered by more than one tile. We, therefore, concatenate all tiles within one unique cycle and pass before further analysis. If a given SWOT pass partially covers lakes, we do not discard it from our analysis, as long as it fulfills the selection criteria described in the following subsections. The PIXC data product contains many targets that can have vastly different WSEs at proximity. To minimize their influence, we extract the PIXC observations via the lake mask.

3.2 Water Surface Elevation

The SWOT WSE w.r.t. the EGM2008 geoid used in this work (H_{swot}) is based on points with the "open water" class (JPL, 2023b) through the following expression

$$H_{swot}(P) = h(P) - (T_{solid} + T_{load} + T_{pole})(P) - N_{geoid}(P), \quad (1)$$

https://doi.org/10.5194/egusphere-2025-6366
Preprint. Discussion started: 11 February 2026

for one point (P) with the natively reported height (h) given w.r.t. the WGS84 reference ellipsoid (JPL, 2024b), corrected for instrument and crossover calibrations, signal propagation delays due to iono- and troposphere (dry & wet) (JPL, 2023b), all three earth tides (T), and the geoid height above the reference ellipsoid (N_{geoid}). Here we apply the EGM2008 geoid model (Pavlis et al., 2012) provided in the SWOT product.

3.3 Water Level Time Series: Data Selection Criteria

To account for outliers that persist after the spatial masking process, we utilise that SWOT surface elevations within one lake are approximately normal–distributed. Therefore, an observation P (one point) is excluded if it is outside the 99.7% confidence interval

$$H_{swot}(P) \notin [\mu - 3\sigma, \mu + 3\sigma](H_{swot}), \tag{2}$$

with mean (μ) and standard deviation (σ) of the lake surface elevations H_{swot} for the respective acquisition. From this stage, we defined and tested six data selection criteria to understand which observation points should be used to summarize the WSE for the given timestamp. The criteria are presented in Table 1. We chose the median over the mean as the summary measure of the water level since it is more robust to outliers that might be missed by previous filtering. The median is applied to all available points or to points without a geo–flag. Where geo–flag refers to the point–wise 32bit geolocation quality flag indicating the quality of variables such as elevation h, latitude, and longitude. We use the geolocation quality flag over the other available quality flags, as it is the designated quality flag for e.g. *height* in the SWOT documentation (JPL, 2023b).

The median WSE for a given timestamp and lake can be discarded based on WSE standard deviation, the number of points used for the median, or if too many points are geo–flagged. We found that acquisitions with fewer than 200 points produced outliers in the time series. Generally, no lake is completely discarded based on the data selection criteria; it is strictly applied to the individual timestamps in the time series. Hence, if one lake's acquisition is discarded based on having fewer than 200 points, only that particular timestamp will be missing in the final time series.

Table 1. Data selection criteria describing how to aggregate one WSE measure for a given lake and timestamp, and when to discard it.

Selection Criteria	Summary Measure	on which Points	min N of Points for timestamp	std
1	median	all	–	–
2	median	all	200	–
3	median	all	200	$\leq$1
4	median	all if max 20% geo–flagged	200	$\leq$1
5	median	points without geo–flag	–	–
6	median	points without geo–flag	200	–

https://doi.org/10.5194/egusphere-2025-6366
Preprint. Discussion started: 11 February 2026

3.4 Offset and Errors

The SWOT and gauge–based WSE time series have a constant offset, given the different vertical references. In addition, the SWOT KaRIn measurements are sensitive to errors in the roll angle and interferometric phase (JPL, 2024b), which are addressed in the satellite crossover calibration. Hence, potential errors in the crossover correction might introduce additional, time–varying errors between the gauge and SWOT–based water level time series, similarly to what has been shown for the ocean (Jacobs et al., 2025). Hence, if present, a remaining roll error at a given time stamp would result in a larger error, between the gauge and SWOT WSE in one side of the swath and a smaller one in the other side. Danish lakes typically have seasonal WSE variations of less than 1m, thus, even minor remaining crossover correction errors would influence the time series. We see the possibility for a time–varying **residual roll error** (ϵ_{roll}) that is a function of the lake's position relative to the ground track of SWOT – similarly to a "slope". SWOT's errors and in particular also roll error are discussed by Peral and Esteban-Fernandez (2018); Peral et al. (2024).

To report sensible metrics for relative WSE change, the constant offset per lake must be removed. The difference in WSE (ΔH) between the gauge (H_{gauge}) and SWOT is given by

$$\Delta H(id,c,p) = H_{gauge}(id,c,p) - H_{swot}(id,c,p), \tag{3}$$

with data for all cycles (c) and passes (p) for the respective lake (id), if gauge data is available and valid surface elevations H_{swot} following the selection criteria of Section 3.3 exist. The constant offset per lake (b_-) is then computed as

$$b_-(id) = median(\Delta H(id,c,p)), \quad \Rightarrow \quad \Delta H' = H_{gauge} - b_- - H_{swot}. \tag{4}$$

The roll error depends on the lake's distance to SWOT's ground track ($d \in [-60, 60]$km). We use the lake's centroid and define negative distances to the left of SWOT's ground track. If roll errors are present, we expect a correlation between the gauge–SWOT difference $\Delta H'$ and the perpendicular ground track distance (d). The correlation is significant if the p–value is ≤ 0.05. If this is the case and the $|\text{PCC}| \geq 0.7$, we classify the acquisition to have a roll error. The error budget is superimposed with random noise ϵ_{random} for each lake. The total error is hence conceptually described as

$$\Delta H(id,c,p) = b_-(id) + d \cdot \epsilon_{roll}(c,p) + \epsilon_{random}(id,c,p). \tag{5}$$

We expect the residual roll error to occur only in some of SWOT's acquisitions and to be small. We investigate indications of the error over Danish lakes, while the main focus remains on evaluating SWOT's capability to detect relative WSE changes in small Danish lakes.

3.5 Statistical Evaluation with Gauges

The water level time series are evaluated per lake against gauge data using the Root Mean Square Error (RMSE) and Pearson Correlation Coefficient (PCC), defined as:

$$RMSE = \sqrt{\frac{1}{N}\sum (x_i - y_i)^2}, \quad PCC = \frac{\sum (x_i - \bar{x})(y_i - \bar{y})}{\sqrt{\sum (x_i - \bar{x})^2 \sum (y_i - \bar{y})^2}} \in [-1, 1], \tag{6}$$

https://doi.org/10.5194/egusphere-2025-6366
Preprint. Discussion started: 11 February 2026

with SWOT estimated water level (x), target offset removed gauge water level (y), and $\bar{x}$ / $\bar{y}$ represent the mean. x is formed from H_{swot}, potentially with added corrections. Danish lakes typically have small seasonal signals ($<$ 1m in 2023/24), deteriorating the expressiveness of the RMSE. Hence, it is important to consider both RMSE and correlation simultaneously.

4 Results

4.1 Time Series Data Selection Criteria

The time series for the six defined data selection criteria (Table 1) are shown in Figure 2 for Valsølille Sø, a typical Danish lake w.r.t. surface area and seasonal signal. The offset removed gauge timeseries is exemplary shown for criteria 6. The results for all gauged lakes are summarised in Table 2. Requiring a minimum of 200 observations shows good improvements in RMSE and PCC, while the requirement for the standard deviation shows no improvement. Requiring a maximum of 20% of geo-flagged points significantly improves the scores. Excluding all geo-flagged points yields similar results. Criterion 6, which requires a minimum of 200 observations per lake and timestamp, performs equally to criterion 4 but does not contain flagged points. Therefore, we adopt criterion 6 for the remainder of this paper as the more conservative criterion. The LakeSP time series exhibits good RMSE and PCC, but retains significantly fewer valid timestamps compared to criterion 6.

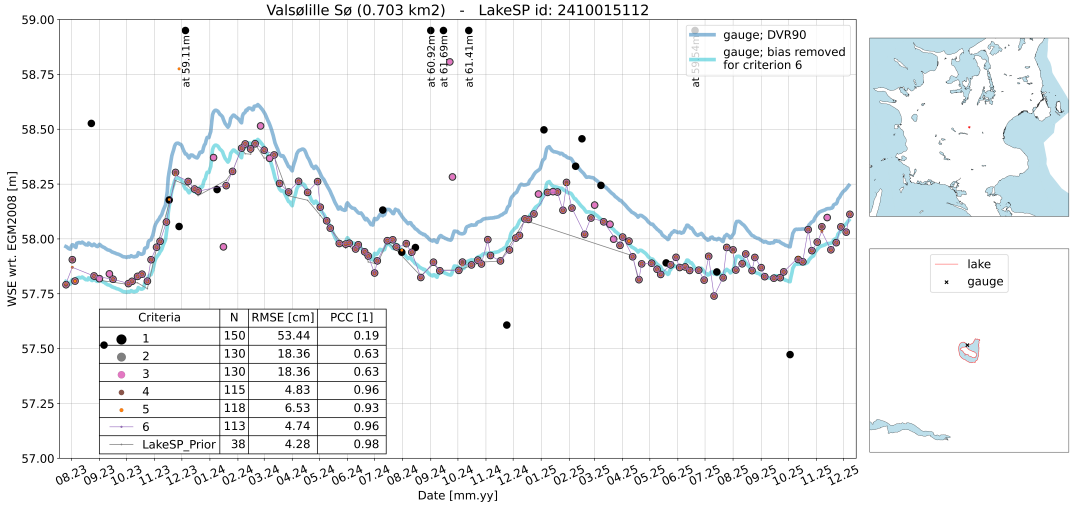

Figure 2. SWOT WSE time series for all 6 defined data selection criteria, exemplary for Valsølille Sø, with RMSE and Pearson Correlation Coefficient vs. gauge data and the number of timestamps in the respective time series (N). Filtered LakeSP prior data is shown for reference.

4.2 Roll Error

Figure 3A shows the height difference between the offset removed gauge and SWOT ($\Delta H'$) for lakes observed by pass 152 over all cycles. Up to 19 lakes are observed by SWOT in this pass. The number might be lower in the individual cycles due to

https://doi.org/10.5194/egusphere-2025-6366
Preprint. Discussion started: 11 February 2026

Table 2. Median and 2.5% / 97.5% quantiles of the root mean square error [cm] and Pearson correlation coefficient [1] of all 37 used gauged lakes for the 6 time series data selection criteria. Summary metrics are described in Table 1.

Summary metric	1	2	3	4	5	6
2.5% quantile	7.95	6.24	5.74	4.09	4.12	4.14
median RMSE	26.76	13.79	13.07	5.16	7.33	5.34
97.5% quantile	618.50	232.09	53.58	17.39	452.21	18.37
2.5% quantile	−0.06	0.00	0.10	0.37	−0.13	0.36
median PCC	0.42	0.57	0.63	0.93	0.81	0.91
97.5% quantile	0.94	0.97	0.97	0.99	0.99	0.99

the selection criteria. In this pass, SWOT observes lakes in two hydrologically separate areas. Lakes in Jutland are shown in blue and lakes outside Jutland in red. All lakes outside of Jutland are to the left of the SWOT ground track, while all but one Jutlandic lake are to the right of SWOT's ground track. The distribution of $\Delta H'$ as a function of cycle is generally centered around zero, yet some cycles display a slight offset. Cycles with a significant roll component are highlighted by a gray bar. Here, the $\Delta H'$ distributions for lakes in the right and left swath of SWOT show considerable differences. Three cycles with a significant roll component are shown in detail in Figure 3B-D, plotting $\Delta H'$ as a function of the distance to SWOT's ground track. The slope is not constant over time and can change direction. We use the 1σ spread of the time stamp's $\Delta H'$ distribution – shown in green in each plot – as a measure for the roll error amplitude.

Figure 4A analogously shows SWOT's error vs. gauge data for all passes covering Denmark. The median $\Delta H'$ and 1σ quantile spread ($84.15\% - 15.85\%$ quantile) are shown in green if the acquisition has a significant roll error component and in blue if not. For two acquisitions without significant roll error, $\Delta H'$ over d are shown Figure A1G and H. Only acquisitions with a minimum of 10 observed lakes are shown with median and quantile spread to minimize random effects. Of the 127 acquisitions with 10 or more lakes, 23 (ca. 18%) have a significant roll error component. Figure 4B and D show the median of the absolute $\Delta H'$ distribution for acquisitions with and without a significant roll error component. Both are within margin to each other for the lakes investigated in this study. Figure 4C and E show the distribution of 1σ quantile $\Delta H'$ spread for roll and no roll error component. As expected, the comparison reveals a more extensive spread for acquisitions with a significant roll error component. Aggregating Figure 4B and D, the median $|\text{median}(\Delta H')|$ for all acquisition distributions is 2.15cm. The spread for all acquisitions based on Figure 4C and E has a median of 5.68cm, but ranges to 11.29cm for the 0.95 quantile.

4.3 Final Time Series

Three water level time series plots corrected for the constant offset are shown in Figure 5 along with LakeSP based time series. Søby Sø (0.709km^2 surface area, Figure 5B) is an example of a lake with minimal WSE amplitude. The correlation is poor, and the lake's WSE signal appears to be inside of SWOT's error budget. Tivolisøen (0.269km^2 surface area, Figure 5A) is the smallest gauged lake in the study and has a WSE amplitude above 150cm. Despite its size, RMSE (7.10cm) and PCC (0.99) are satisfactory, proving SWOT's capabilities. Mossø (16.569km^2 surface area, Figure 5C) represents a large lake in the Danish

https://doi.org/10.5194/egusphere-2025-6366
Preprint. Discussion started: 11 February 2026

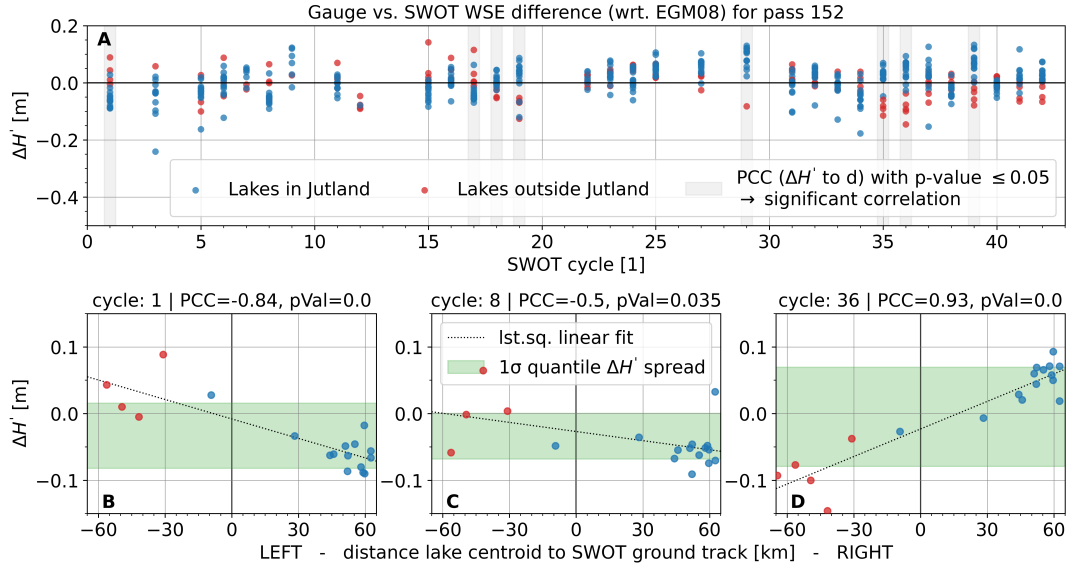

Figure 3. A: $\Delta H'$ (SWOT vs. gauges) over time for all lakes in pass 152. **B-D**: expanded plot of SWOT's error per lake over lake's centroid distance to SWOT's ground track. Negative distances are left and positive to the right of SWOT. Exemplary for the cycles 1, 8, and 12.

context. Here, an overall good SWOT to gauge correlation and a small RMSE is found. For Mossø, we exemplary present a gauge vs. SWOT correlation scatter plot (Figure A1E), showing a linear correlation. For the Danish lakes considered in this study, the LakeSP time series generally shows similar performance to our approach, but retains fewer valid timestamps over the same time period. A detailed list is provided in Table A1. Lakes with high RMSE for the LakeSP data have an outlier that was not removed by the filtering deployed in this study.

The median RMSE for all 37 gauged lakes is 5.34cm with a median PCC of 0.91. Detailed metrics for all lakes are listed in Table A1 and shown in Figure A1A and B in the Appendix. For comparison, the median RMSE for the filtered LakeSP is 6.05cm, and the median PCC is 0.89. The filtered LakeSP (until 02.05.2025) retains a median of 35 timestamps per lake compared to 65 for our data selection criteria. For the whole period until 09.12.2025, our approach retains a median of 98 timestamps for a given lake, shown in Figure A1C.

5 Discussion

5.1 Spatial Masking and LakeSP

This study aims to investigate the relative WSE change. A static lake mask is sufficient for this. If the lake extent expands, the geometry would only mask open water. If the lake shrinks/ disappears/ moves, the mask will include land, too. However, since we only use SWOT's "open water", SWOT's native land exclusion should handle this case. Our requirement for a minimum of 200 points per lake and acquisitions should exclude timestamps with too few observations to form a robust WSE summary.

https://doi.org/10.5194/egusphere-2025-6366
Preprint. Discussion started: 11 February 2026

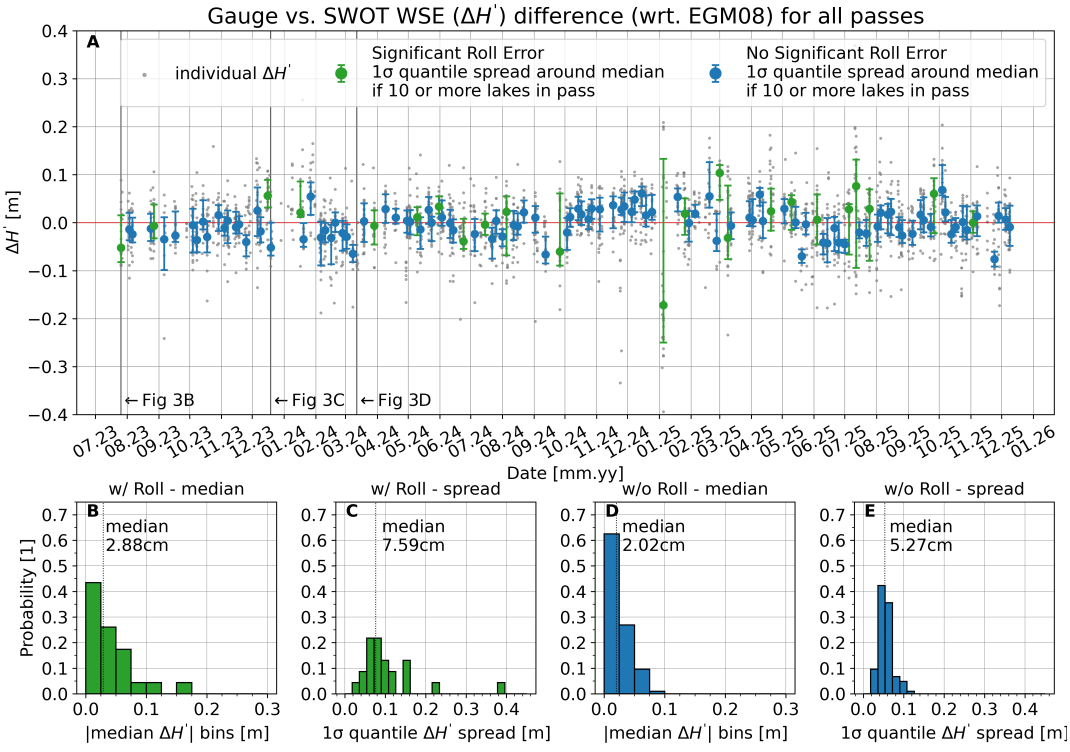

Figure 4. **A**: $\Delta H'$ (SWOT vs. gauges) over time for all passes and all lakes in Denmark. For timestamps with ≥ 10 observed lakes, the median and 1σ quantile spread (0.1585 to 0.8415) are shown. If $\Delta H'$ significantly correlates with distance to SWOT's ground track (d), it is shown in green, otherwise in blue. The three vertical lines indicate the timestamps with detailed correlation plots in Figure 3B-D. **B**: distribution of the absolute median $\Delta H'$ for timestamps with significant roll error. **C**: distribution of the 1σ quantile spread for timestamps with significant roll error. **D**: distribution of the absolute median $\Delta H'$ for timestamps without significant roll error. **E**: distribution of the 1σ quantile spread for timestamps without significant roll error.

In principle, a dynamic mask would be ideal. If it is inaccurate, however, it might introduce noise, as presented in Figure A1F in the Appendix. Measurements of secondary lakes near the target can have significantly different WSE, necessitating robust filtering. Nevertheless, for global applicability, the approach chosen for the LakeSP product should be preferred.

If the LakeSP product is filtered as described above, the LakeSP time series exhibits mostly good RMSE and PCC values, despite the discussed assignment problem. However, this is achieved at the expense of discarding many timestamps that our approach retains, yielding similar or slightly better RMSE and PCC results. For use cases where the temporal resolution is not of the highest priority, but ease of use and computational resources are, we see LakeSP as preferable. The same applies to global products. Quarrying LakeSP from Hydrocron takes seconds per lake. Quarrying the pre–processed aggregated WSE timeseries for a lake from a local database requires a similar time. Pre-processing requires between one and two minutes per pass over Denmark, depending on the number of lakes observed. If the method does not change, this computation has to be

https://doi.org/10.5194/egusphere-2025-6366
Preprint. Discussion started: 11 February 2026

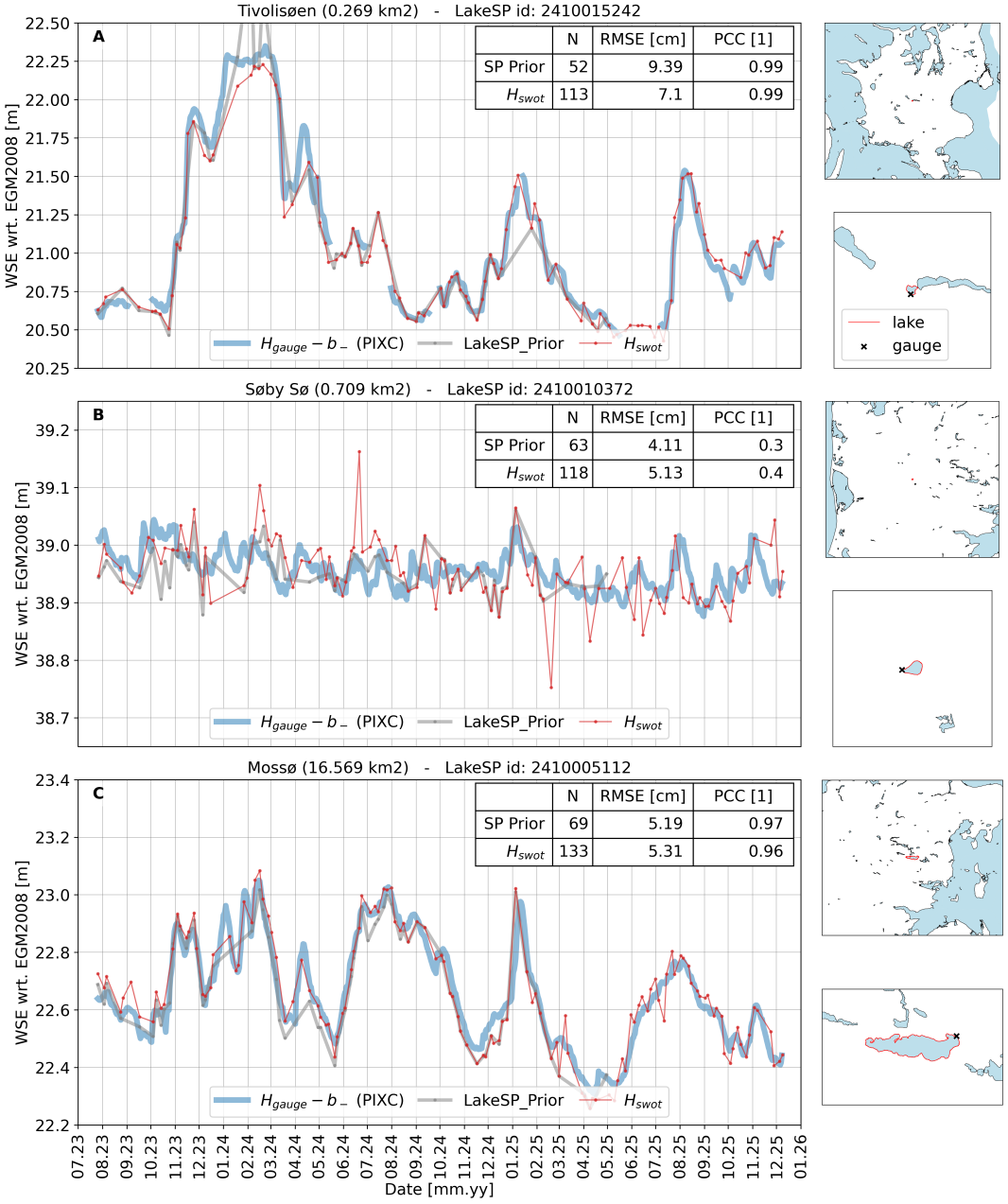

Figure 5. Water surface elevation time series for three typical Danish lakes. Offset removed gauge data is shown in blue, our SWOT approach in red, and filtered SWOT LakeSP Prior time series are shown in the background for comparison. **A** shows Tivolisøen, the smallest lake in this study. **B** shows Søby Sø, a lake with minimal variation in water surface elevation. **C** shows Mossø, the third largest Danish lake.

https://doi.org/10.5194/egusphere-2025-6366
Preprint. Discussion started: 11 February 2026

done only once. Additionally, we need to highlight the different baselines of PIXC to Hydrocron LakeSP. The comparison's details will certainly change with an updated LakeSP baseline; however, the overall conclusion we presented in this paper is consistent with a comparison using only PIXC version C we performed previously. Thus, we have no reason to doubt the presented comparison. Given the rapid advances in SWOT processing, these mismatches can not be avoided.

5.2 Time Series Data Selection Criteria

The results of the data selection criteria showed that the most significant RMSE improvements were achieved from two criteria: 1) requiring a minimum number of SWOT points per acquisition and lake, and 2) posing requirements to the geo–quality–flag. On the other hand, the PCC did not improve significantly from criteria 1 to 2. The overall improvement is mainly attributed to the requirements posed on the geo–flag. It appears that the minor seasonal WSE variations characteristic of Danish lakes can not be resolved appropriately without using the geo-quality flag. Additionally, the marginal difference between criteria 4 to 6 indicates that up to 20% geo–flagged points are not enough to degrade aggregated WSE, at least for the lakes considered here. However, at a conservative choice we recommend to exclude all geo–flagged observations unless the total number of points drops below 200.

This study limited the SWOT observations to the "open water" class, which was sufficient for the lakes investigated in this study. For smaller lakes than those investigated here, it might also be beneficial to consider the "water near land" class. The selection criteria could be further improved by investigating the relationship between individual geo–quality–flags and time series outliers to retain even more valid observation points, as in Bazzi et al. (2025) for the raster product. We were unable to establish a clear relationship in a preliminary investigation. Besides the geo–quality–flag, SWOT provides four additional sets of quality flags that could be used in a model approach. In our preliminary study, we could not observe any added benefit of using other flags besides the geo–quality–flags.

5.3 Performance on Danish Lakes

5.3.1 Timeseries

The aim of this study is to assess SWOT's capability to capture relative changes in WSE in small Danish lakes, rather than absolute elevations. To derive the relevant metrics, we removed the median offset between SWOT and gauge measurements ($b\_$). This adjustment is sufficient for evaluating SWOT's performance in detecting relative WSE changes. Consequently, investigating the origin of the removed offset lies beyond the scope of this study.

The median RMSE of all 37 lakes in this study of 5.34cm, with median PCC of 0.91 is a promising outlook of SWOT's ability to monitor relative WSE changes in small lakes in Denmark and similar regions. Especially considering its high temporal resolution, discussed in the next section. From the three time series shown in Figure 5 we can additionally outline, that a smaller lake area does not necessarily result in worse WSE mapping. The lake's annual amplitude must be considered, too.

https://doi.org/10.5194/egusphere-2025-6366
Preprint. Discussion started: 11 February 2026

5.3.2 Temporal Resolution

At the latitude range of Denmark, SWOT improves the temporal resolution compared to most traditional satellite altimeters. Of the 228 Danish lakes above 0.25km^2, 54.63% are covered by 4 SWOT passes per cycle, 22.47% by 3, and 22.9% by 2, resulting in an average of 3.3 passes per cycle. Accounting for missing acquisitions (we were unable to access 35 out of 417 acquisitions), the average temporal resolution is 9.5 days, slightly less than the theoretical best if all timestamps were provided and would result in a valid WSE value according to our selection criterion. While missions such as Sentinel-6, Jason, etc. achieve a 10-day temporal resolution, their spatial resolution is limited to their 1D ground tracks, which sets a natural threshold to the number of lakes that are measured. SWOT's groundbreaking feature is observing even small lakes at high temporal frequencies.

Downsampling gauge WSE time series to a 9-day resolution yields a median correlation coefficient of 0.96 (2.5%/97.5% quantiles: 0.62/0.99), explaining 0.92 (2.5%/97.5% quantiles: 0.38/0.99) of variability. This demonstrates SWOT's ability to resolve most lake WSE variations in the 37 Danish lakes studied, advancing our understanding of small lake dynamics and providing vital insights for policymakers and communities.

5.4 Roll Error

Based on the lakes investigated in this study and the examples shown in Figure 3 and 4, we find indications of a residual roll error component present in inland SWOT PIXC data. As the sign of the slope is time dependent, illustrated with the cycles of pass 152, we may rule out that the observed slope is related to reference surface issues as this would be constant in time. With the setup of this study, we can not directly quantify the amplitude of the residual roll error, given that random error additionally affects the slope. However, for the lakes investigated in this study, the roll error might be up to $\approx \pm 10$cm near the edge of the swath – for example, in Figure 3D.

The residual roll error can likely be ignored for lakes and other water bodies with large WSE variations. Yet, the error may influence the WSE time series for water bodies with small WSE variations. We think it will be detrimental for future studies using SWOT to be aware of potential residual roll error component and to make a deliberate choice whether addressing it is necessary or not. The residual roll error could be estimated, modeled, and corrected for using either gauge stations or virtual stations at large lakes. A linear approximation could be fitted with as few as 2 stations on either side of SWOT. However, Figure 3B–D shows SWOT's increased error in the far range. This has to be considered when attempting to correct for the roll error component. Overall, more research is required, and future SWOT processing baselines likely will improve on this issue.

6 Conclusions

This study investigated how SWOT PIXC data can be used to generate high–accuracy WSE time series for Danish lakes between 0.25km^2 and 40km^2 surface area and caputre their relative WSE change. By aggregating meta-information for 37 gauged lakes, we established a robust validation dataset for Denmark, providing a solid foundation for evaluating the perfor-

https://doi.org/10.5194/egusphere-2025-6366
Preprint. Discussion started: 11 February 2026

mance of SWOT's altimetry data over the time span from July 2023 to December 2025. We demonstrated that our method performs slightly better than filtered LakeSP data, while retaining more SWOT observation timestamps. Time series based on our approach capture relative WSE change with a median RMSE of 5.34cm and PCC of 0.91 across all 37 lakes. We found a significant roll error component in about 18% of all acquisitions with 10 or more lakes. Without a systematic setup, a quantification of its amplitude is not possible. However, we presented instances for Danish lakes where the residual roll error reaches up to $\pm$10cm.

Overall, SWOT provides unprecedented data, enabling the construction of high-temporal-resolution and high-accuracy WSE time series that were previously unattainable. This is especially impactful for smaller lakes, which are now likely observed by a satellite altimeter for the first time, due to SWOT's broad spatial coverage, compared to traditional satellite altimeter's ground track data.

Data availability. Our data is hosted at DTU DATA (Köhn and Nielsen, 2025). The complete processed SWOT data set with all auxiliary information is available as a SQL source file. We used `MariaDB` 11.3 and `HeidiSQL` 12.6 for set–up and management, and the Python `mariadb` package for access. Data associated with Table A1 are available as separate EXCEL files.

Raw SWOT HR PIXC 2.0 data (SWOT, 2024b) was downloaded using the Python `earthaccess` API (Barrett et al., 2024). Gauge data was accessed via Vandportalen (WSP, 2024) and SWOT HR LakeSP Prior data via the Hydrocron API (Greguska et al., 2025). Lake vector geometries for masking SWOT data are taken from Geo Danmark 60 (@geodanmark, 2024) documented in GeoDanmark (2018).

Appendix A: Supporting Figures

https://doi.org/10.5194/egusphere-2025-6366
Preprint. Discussion started: 11 February 2026

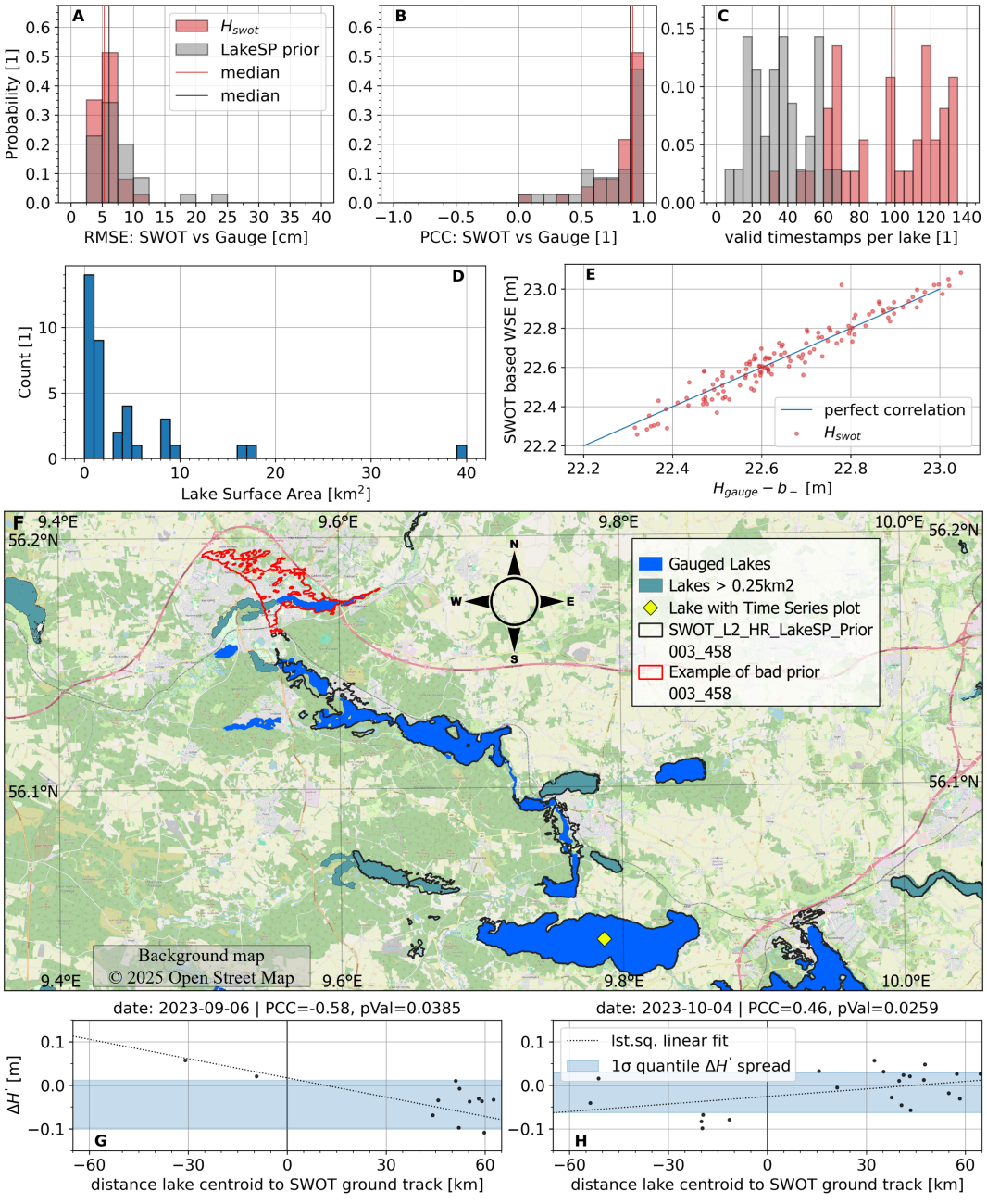

Figure A1. A and **B**: RMSE and PCC for SWOT vs. bias removed gauge WSE for our approach and filtered LakeSP Prior. Using all available lakes. **C**: valid SWOT time stamps retained for our approach and the filtered LakeSP prior. **D**: distribution of lake surface area of all 37 lakes in this study. **E**: correlation scatter plot for Mossø, shown in Figure 5C. **F**: Example of prior problem in LakeSP for Danish lakes around Viborg. **G** and **H**: Example of two acquisition without significant residual roll error: error over distance to SWOT ground track.

https://doi.org/10.5194/egusphere-2025-6366
Preprint. Discussion started: 11 February 2026

Appendix B: Table of Gauged Lakes

https://doi.org/10.5194/egusphere-2025-6366
Preprint. Discussion started: 11 February 2026

Table A1. List of all used gauged Danish lakes (lager than 0.25km^2) †: Lake with time series plot. *: relative metrics for H_{swot} (this paper's approach). **: relative metrics for LakeSP Prior (a dedicated offset is computed). b_{-}: gauge offset wrt. H_{swot}. N: number of SWOT based time series timestamps; for PIXC until 09.12.25 and for LakeSP until 02.05.25. ΔWSE: max. amplitude of WSE from gauge data.

name	LakeSP id	Area	gauge lon & lat		b_{-}	ΔWSE	RMSE [cm]		PCC [1]		N [1]	
N=37		[km^2]	[deg]	[deg]	[cm]	[cm]	*	**	*	**	*	**
Arresø	2410015352	39.547	12.0403	55.9778	17.06	40.2	8.14	8.24	0.71	0.7	123	58
Brabrand Sø	2410005882	1.459	10.0888	56.1477	20.88	198.5	7.52	9.0	0.99	0.99	61	26
Brassø	2410004442	1.215	9.5591	56.1472	12.42	40.1	89.26	11.99	-0.0	0.74	116	31
Byrup Langsø	2410004542	0.365	9.5169	56.0213	8.56	60.9	6.0	8.26	0.94	0.89	49	17
Engelsholm Sø	2410005242	0.429	9.3209	55.7166	14.22	35.5	5.68	5.2	0.73	0.84	107	49
Esrum Sø	2410014592	17.37	12.3807	56.0363	14.1	62.4	7.74	4.22	0.88	0.94	96	24
Filsø (S)	2410011002	4.173	8.2075	55.7005	16.33	106.2	4.16	5.36	0.98	0.96	65	33
Flyndersø	2410026512	4.799	8.9603	56.5203	6.15	28.1	5.94	6.72	0.61	0.01	69	31
Furesø	2410014642	9.351	12.461	55.8105	15.6	29.3	4.61	7.98	0.69	0.58	96	19
Fårup Sø	2410010292	0.958	9.4176	55.7369	14.6	53.6	5.25	6.38	0.89	0.87	119	53
Grynderup Sø	2410026362	1.275	8.9517	56.7961	-6.03	66.2	6.0	23.63	0.81	0.74	33	17
Gudensø	2410005972	1.682	9.7452	56.0618	12.35	38.6	4.8	10.33	0.86	0.55	127	36
Hinge Sø	2410024582	0.916	9.5287	56.2648	-10.1	71.0	5.05	8.54	0.93	0.9	117	58
Julsø	2130011152	8.451	9.6483	56.1202	13.75	47.8	4.23	51.27	0.91	0.42	132	8
Kimmerslev Sø	2410016382	0.377	11.9821	55.4862	9.79	85.5	6.46	90.33	0.94	0.67	80	18
Mossø †	2410005112	16.569	9.849	56.0482	15.69	74.2	5.31	5.19	0.96	0.97	133	69
None	2410011012	0.827	8.2234	56.1889	14.27	81.5	5.34	19.2	0.89	0.54	79	22
Ovesø	2410023522	3.725	8.4014	56.8889	17.28	167.5	5.36	5.03	0.99	0.99	68	38
Ravnsø	2410005102	1.791	9.8232	56.1038	12.56	84.6	4.7	5.46	0.97	0.97	126	56
Silkeborg Langsø (east)	2410005722	1.061	9.6003	56.1738	10.48	118.1	4.46	8.83	0.99	0.96	98	40
Skanderborg Sø	2410006032	8.646	9.9349	56.0341	13.59	93.2	5.69	5.94	0.97	0.96	101	24
Slivsø	2410005352	1.688	9.46	55.1816	23.65	108.3	6.56	3.75	0.96	0.98	63	30
Stevning Dam	2410007182	0.288	9.3734	55.2385	17.33	63.3	10.49	3.06	0.61	0.96	73	15
Store Kattinge Sø	–	0.667	12.0244	55.6558	11.73	36.4	6.32	–	0.8	–	117	–
Stubbe Sø	2410024832	3.717	10.7223	56.2551	12.23	37.7	6.2	4.73	0.81	0.78	127	39
Søby Sø †	2410010372	0.709	9.0562	56.0483	7.47	16.8	5.13	4.11	0.4	0.3	118	63
Søndersø (Maribo)	–	8.075	11.4912	54.7569	17.18	71.9	6.12	–	0.93	–	61	–
Tange Sø	2410024672	5.428	9.5969	56.3111	10.91	40.6	3.92	5.78	0.84	0.55	132	56
Thorsø	2410005082	0.693	9.5576	56.1281	13.81	30.6	5.44	6.1	0.53	0.65	95	24
Tivolisøen †	2410015242	0.269	11.7442	55.4787	20.26	188.5	7.1	9.39	0.99	0.99	113	52
Tuelsø	2410015252	1.877	11.6014	55.4443	9.72	84.4	4.16	5.92	0.98	0.97	130	59
Valsølille Sø †	2410015112	0.703	11.8469	55.523	15.9	69.7	4.74	4.28	0.96	0.98	113	38
Vandet Sø	2410025112	4.783	8.5813	57.0058	14.09	74.9	4.37	3.54	0.98	0.97	69	35
Vandkraftsøen	2410025962	0.639	8.6389	56.3516	12.08	49.4	4.19	180.99	0.75	0.39	53	14
Vedsø	2410025832	1.497	9.4287	56.3996	7.13	20.6	4.56	11.93	0.55	0.15	120	42
Ørnsø	2410005052	0.404	9.5147	56.157	9.87	146.7	5.09	4.85	0.98	0.99	83	28
Ørum Sø	2410023442	4.447	8.2908	56.7931	20.32	103.5	4.97	5.31	0.97	0.95	69	40

https://doi.org/10.5194/egusphere-2025-6366
Preprint. Discussion started: 11 February 2026

Author contributions. KN and SK conceptualized the study, SK performed the code development and data acquisition and harmonization. SK prepared the manuscript with contributions from all co-authors.

Competing interests. The authors declare that they have no conflict of interest.

Acknowledgements. We would like to thank Klimadatastyrelsen (KDS), for supporting our research. Furthermore, we thank Miljøstyrelsen, HOFOR, and Aarhus, Haderslev, Halsnæs, Lolland, Næstved, Ringkøbing–Skjern, Ringsted, Roskilde, Skanderborg, Silkeborg, Thisted, and Vejle– Kommune, as well as Aage V. Jensen Naturfond, Nationalpark Kongernes Nordsjælland, Vestforsyning A/S, and WSP for making their gauge data openly accessible on Vandportalen, and thus to allow us to validate SWOT's capabilities. Furthermore, all the other municipalities and operators whose gauges we didn't use for this work. Finally, we acknowledge Colin Gleason and Curtis Chen for input to the paper during review. Last but not least, the anonymous reviewers for greatly improving this manuscript.

During the writing of this article, LLMs were occasionally used to improve readability of smaller sections. The contents were carefully monitored and altered by the authors.

https://doi.org/10.5194/egusphere-2025-6366
Preprint. Discussion started: 11 February 2026

References

Abdalla, S., Abdeh Kolahchi, A., Ablain, M., Adusumilli, S., Aich Bhowmick, S., Alou-Font, E., Amarouche, L., Andersen, O. B., Antich, H., Aouf, L., Arbic, B., Armitage, T., Arnault, S., Artana, C., Aulicino, G., Ayoub, N., Badulin, S., Baker, S., Banks, C., Bao, L., Barbetta, S., Barceló-Llull, B., Barlier, F., Basu, S., Bauer-Gottwein, P., Becker, M., Beckley, B., Bellefond, N., Belonenko, T., Benkiran, M., Benkouider, T., Bennartz, R., Benveniste, J., Bercher, N., Berge-Nguyen, M., Bettencourt, J., Blarel, F., Blazquez, A., Blumstein, D., Bonnefond, P., Borde, F., Bouffard, J., Boy, F., Boy, J.-P., Brachet, C., Brasseur, P., Braun, A., Brocca, L., Brockley, D., Brodeau, L., Brown, S., Bruinsma, S., Bulczak, A., Buzzard, S., Cahill, M., Calmant, S., Calzas, M., Camici, S., Cancet, M., Capdeville, H., Carabajal, C. C., Carrere, L., Cazenave, A., Chassignet, E. P., Chauhan, P., Cherchali, S., Chereskin, T., Cheymol, C., Ciani, D., Cipollini, P., Cirillo, F., Cosme, E., Coss, S., Cotroneo, Y., Cotton, D., Couhert, A., Coutin-Faye, S., Crétaux, J.-F., Cyr, F., d'Ovidio, F., Darrozes, J., David, C., Dayoub, N., De Staerke, D., Deng, X., Desai, S., Desjonqueres, J.-D., Dettmering, D., Di Bella, A., Díaz-Barroso, L., Dibarboure, G., Dieng, H. B., Dinardo, S., Dobslaw, H., Dodet, G., Doglioli, A., Domeneghetti, A., Donahue, D., Dong, S., Donlon, C., Dorandeu, J., Drezen, C., Drinkwater, M., Du Penhoat, Y., Dushaw, B., Egido, A., Erofeeva, S., Escudier, P., Esselborn, S., Exertier, P., Fablet, R., Falco, C., Farrell, S. L., Faugere, Y., Femenias, P., Fenoglio, L., Fernandes, J., Fernández, J. G., Ferrage, P., Ferrari, R., Fichen, L., Filippucci, P., Flampouris, S., Fleury, S., Fornari, M., Forsberg, R., Frappart, F., laure Frery, M., Garcia, P., Garcia-Mondejar, A., Gaudelli, J., Gaultier, L., Getirana, A., Gibert, F., Gil, A., Gilbert, L., Gille, S., Giulicchi, L., Gómez-Enri, J., Gómez-Navarro, L., Gommenginger, C., Gourdeau, L., Griffin, D., Groh, A., Guerin, A., Guerrero, R., Guinle, T., Gupta, P., Gutknecht, B. D., Hamon, M., Han, G., Hauser, D., Helm, V., Hendricks, S., Hernandez, F., Hogg, A., Horwath, M., Idžanović, M., Janssen, P., Jeansou, E., Jia, Y., Jia, Y., Jiang, L., Johannessen, J. A., Kamachi, M., Karimova, S., Kelly, K., Kim, S. Y., King, R., Kittel, C. M., Klein, P., Klos, A., Knudsen, P., Koenig, R., Kostianoy, A., Kouraev, A., Kumar, R., Labroue, S., Lago, L. S., Lambin, J., Lasson, L., Laurain, O., Laxenaire, R., Lázaro, C., Le Gac, S., Le Sommer, J., Le Traon, P.-Y., Lebedev, S., Léger, F., Legresy, B., Lemoine, F., Lenain, L., Leuliette, E., Levy, M., Lillibridge, J., Liu, J., Llovel, W., Lyard, F., Macintosh, C., Makhoul Varona, E., Manfredi, C., Marin, F., Mason, E., Massari, C., Mavrocordatos, C., Maximenko, N., McMillan, M., Medina, T., Melet, A., Meloni, M., Mertikas, S., Metref, S., Meyssignac, B., Minster, J.-F., Moreau, T., Moreira, D., Morel, Y., Morrow, R., Moyard, J., Mulet, S., Naeije, M., Nerem, R. S., Ngodock, H., Nielsen, K., Øie Nilsen, J. E., Niño, F., Nogueira Loddo, C., Noûs, C., Obligis, E., Otosaka, I., Otten, M., Oztunali Ozbahceci, B., P. Raj, R., Paiva, R., Paniagua, G., Paolo, F., Paris, A., Pascual, A., Passaro, M., Paul, S., Pavelsky, T., Pearson, C., Penduff, T., Peng, F., Perosanz, F., Picot, N., Piras, F., Poggiali, V., Étienne Poirier, Ponce de León, S., Prants, S., Prigent, C., Provost, C., Pujol, M.-I., Qiu, B., Quilfen, Y., Rami, A., Raney, R. K., Raynal, M., Remy, E., Rémy, F., Restano, M., Richardson, A., Richardson, D., Ricker, R., Ricko, M., Rinne, E., Rose, S. K., Rosmorduc, V., Rudenko, S., Ruiz, S., Ryan, B. J., Salaün, C., Sanchez-Roman, A., Sandberg Sørensen, L., Sandwell, D., Saraceno, M., Scagliola, M., Schaeffer, P., Scharffenberg, M. G., Scharroo, R., Schiller, A., Schneider, R., Schwatke, C., Scozzari, A., Ser-giacomi, E., Seyler, F., Shah, R., Sharma, R., Shaw, A., Shepherd, A., Shriver, J., Shum, C., Simons, W., Simonsen, S. B., Slater, T., Smith, W., Soares, S., Sokolovskiy, M., Soudarin, L., Spatar, C., Speich, S., Srinivasan, M., Srokosz, M., Stanev, E., Staneva, J., Steunou, N., Stroeve, J., Su, B., Sulistioadi, Y. B., Swain, D., Sylvestre-baron, A., Taburet, N., Tailleux, R., Takayama, K., Tapley, B., Tarpanelli, A., Tavernier, G., Testut, L., Thakur, P. K., Thibaut, P., Thompson, L., Tintoré, J., Tison, C., Tourain, C., Tournadre, J., Townsend, B., Tran, N., Trilles, S., Tsamados, M., Tseng, K.-H., Ubelmann, C., Uebbing, B., Vergara, O., Verron, J., Vieira, T., Vignudelli, S., Vinogradova Shiffer, N., Visser, P., Vivier, F., Volkov, D., von Schuckmann, K., Vuglinskii, V., Vuilleumier, P., Walter, B., Wang, J., Wang, C., Watson, C., Wilkin, J., Willis, J., Wilson, H., Woodworth, P., Yang, K., Yao, F., Zaharia, R., Zakharova, E., Zaron, E. D., Zhang, Y., Zhao, Z.,

https://doi.org/10.5194/egusphere-2025-6366
Preprint. Discussion started: 11 February 2026

Zinchenko, V., and Zlotnicki, V.: Altimetry for the future: Building on 25 years of progress, Advances in Space Research, 68, 319–363, https://doi.org/https://doi.org/10.1016/j.asr.2021.01.022, 25 Years of Progress in Radar Altimetry, 2021.

Barrett, A., Battisto, C., Bourbeau, J., Fisher, M., Kaufman, D., Kennedy, J., Lopez, L., Lowndes, J., Scheick, J., and Steiker, A.: earthaccess, https://doi.org/10.5281/zenodo.13871886, 2024.

Bazzi, H., Baghdadi, N., Ngo, Y.-N., Normandin, C., Frappart, F., and Cazals, C.: Assessing SWOT interferometric SAR altimetry for inland water monitoring: insights from Lake Léman, Frontiers in Remote Sensing, Volume 6 - 2025, https://doi.org/10.3389/frsen.2025.1572114, 2025.

Best, J.: Anthropogenic stresses on the world's big rivers, Nature Geoscience, 12, 7–21, https://doi.org/https://doi.org/10.1038/s41561-018-0262-x, 2019.

Biancamaria, S., Lettenmaier, D. P., and Pavelsky, T. M.: The SWOT Mission and Its Capabilities for Land Hydrology, pp. 117–147, Springer International Publishing, Cham, ISBN 978-3-319-32449-4, https://doi.org/10.1007/978-3-319-32449-4_6, 2016.

Birkett, C., Reynolds, C., Beckley, B., and Doorn, B.: From Research to Operations: The USDA Global Reservoir and Lake Monitor, pp. 19–50, Springer Berlin Heidelberg, Berlin, Heidelberg, ISBN 978-3-642-12796-0, https://doi.org/10.1007/978-3-642-12796-0_2, 2011.

Buzzanga, B., Hamlington, B. D., Bekaert, D. P. S., Pavelsky, T., Handwerger, A., Bonnema, M., and Lee, C.: Monitoring Water From Space: An Illustration in Death Valley, California, Geophysical Research Letters, 52, e2024GL110 250, https://doi.org/https://doi.org/10.1029/2024GL110250, e2024GL110250 2024GL110250, 2025.

Carrea, L., Cretaux, J., Liu, X., Wu, Y., Berge-Nguyen, M., Calmettes, B., Duguay, C., Jiand, D., Merchant, C., Mueller, D., Selmes, N., Simis, S., Spyrakos, E., Stelzer, K., Warren, M., Yesou, H., and Zhang, D.: ESA Lakes Climate Change Initiative (Lakes_cci): Lake products, Version 2.1., NERC EDS Centre for Environmental Data Analysis, https://doi.org/doi:10.5285/7fc9df8070d34cacab8092e45ef276f1, 2024.

Cole, J. J., Caraco, N. F., Kling, G. W., and Kratz, T. K.: Carbon Dioxide Supersaturation in the Surface Waters of Lakes, Science, 265, 1568–1570, https://doi.org/10.1126/science.265.5178.1568, 1994.

Copernicus: Copernicus Land Monitoring Service: Water Bodies, https://land.copernicus.eu/en/products/water-bodies, accessed: 09.09.2024, 2024.

Crétaux, J.-F., Arsen, A., Calmant, S., Kouraev, A., Vuglinski, V., Bergé-Nguyen, M., Gennero, M.-C., Nino, F., Abarca Del Rio, R., Cazenave, A., and Maisongrande, P.: SOLS: A lake database to monitor in the Near Real Time water level and storage variations from remote sensing data, Advances in Space Research, 47, 1497–1507, https://doi.org/https://doi.org/10.1016/j.asr.2011.01.004, 2011.

DMI: Manual for marine vandstandsmålere, https://www.dmi.dk/fileadmin/user_upload/Bruger_upload/Nyhed/2018/11/Vandstandsmaalermanual_2018.pdf, accessed: 28.03.2025, 2018.

ESA: ESA climate Office: Lakes, https://climate.esa.int/en/projects/lakes/, accessed: 09.09.2024, 2024.

Fjørtoft, R., Gaudin, J.-M., Pourthié, N., Lalaurie, J.-C., Mallet, A., Nouvel, J.-F., Martinot-Lagarde, J., Oriot, H., Borderies, P., Ruiz, C., and Daniel, S.: KaRIn on SWOT: Characteristics of Near-Nadir Ka-Band Interferometric SAR Imagery, IEEE Transactions on Geoscience and Remote Sensing, 52, 2172–2185, https://doi.org/10.1109/TGRS.2013.2258402, 2014.

Fu, L.-L., Pavelsky, T., Cretaux, J.-F., Morrow, R., Farrar, J. T., Vaze, P., Sengenes, P., Vinogradova-Shiffer, N., Sylvestre-Baron, A., Picot, N., and Dibarboure, G.: The Surface Water and Ocean Topography Mission: A Breakthrough in Radar Remote Sensing of the Ocean and Land Surface Water, Geophysical Research Letters, 51, e2023GL107 652, https://doi.org/https://doi.org/10.1029/2023GL107652, e2023GL107652 2023GL107652, 2024.

GeoDanmark: Specifikation 6.0 2018.1114, http://geodanmark.nu/Spec6/HTML5/DK/StartHer.htm, accessed: 31.07.2024, 2018.

https://doi.org/10.5194/egusphere-2025-6366
Preprint. Discussion started: 11 February 2026

@geodanmark: CC BY 4.0 licens gælder for GeoDanmark grunddata og de Geografiske fagdata i GeoDanmark, https://www.geodanmark.dk/home/vejledninger/vilkaar-for-data-anvendelse/, accessed: 30.10.2024, 2024.

Greguska, F., Tebaldi, N., McDonald, V., Vanesa, Nickles, C., and Wood, J.: podaac/hydrocron: 1.6.4, https://doi.org/10.5281/zenodo.15831782, 2025.

Jacobs, G., D'Addezio, J., and Bartels, B.: SWOT Cross-Track Error Characteristics Estimated From Observations, Journal of Geophysical Research: Oceans, 130, e2024JC021 535, https://doi.org/https://doi.org/10.1029/2024JC021535, e2024JC021535 2024JC021535, 2025.

JPL: SWOT Product Description Document Long Name: Level 2 KaRIn High Rate Lake Single Pass Vector Product Short Name: L2_HR_LakeSP, Internal document, Jet Propulsion Laboratory, Pasadena, CA, https://podaac.jpl.nasa.gov/dataset/SWOT_L2_HR_LakeSP_2.0, 2023a.

JPL: SWOT Product Description Document: Level 2 KaRIn High Rate Water Mask Pixel Cloud (L2_HR_PIXC) Data Product, Internal Document JPL D-56411 Revision B, Jet Propulsion Laboratory, Pasadena, CA, https://podaac.jpl.nasa.gov/dataset/SWOT_L2_HR_PIXC_2.0, 2023b.

JPL: SWOT mission overview, https://swot.jpl.nasa.gov/mission/overview/, accessed: 11.09.2024, 2024a.

JPL: SWOT Science Data Products User Handbook, Internal Document JPL D-109532, Jet Propulsion Laboratory, Pasadena, CA, https://podaac.jpl.nasa.gov/dataset/SWOT_L2_HR_PIXC_2.0, 2024b.

JPL/NASA: SWOT Science Orbit, https://swot.jpl.nasa.gov/resources/89/swot-science-orbit/, accessed: 11.09.2024, 2019.

KDS: GeoDanmark-grunddata, https://www.klimadatastyrelsen.dk/vores-opgaver/kortlaegning-og-geodata/geodanmark-grunddata, accessed: 07.10.2024, 2024.

Köhn, S. J. and Nielsen, K.: Evaluation of SWOT HR PIXC 2.0 water level time series of small lakes - Dataset, https://doi.org/10.11583/DTU.27100375, [Dataset], 2025.

Laipelt, L., de Paiva, R. C. D., Fan, F. M., Collischonn, W., Papa, F., and Ruhoff, A.: SWOT Reveals How the 2024 Disastrous Flood in South Brazil Was Intensified by Increased Water Slope and Wind Forcing, Geophysical Research Letters, 52, e2024GL111 287, https://doi.org/https://doi.org/10.1029/2024GL111287, e2024GL111287 2024GL111287, 2025.

Lehner, B. and Döll, P.: Development and validation of a global database of lakes, reservoirs and wetlands, Journal of Hydrology, 296, 1–22, https://doi.org/https://doi.org/10.1016/j.jhydrol.2004.03.028, 2004.

Pavlis, N. K., Holmes, S. A., Kenyon, S. C., and Factor, J. K.: The development and evaluation of the Earth Gravitational Model 2008 (EGM2008), Journal of Geophysical Research: Solid Earth, 117, https://doi.org/https://doi.org/10.1029/2011JB008916, 2012.

Peral, E. and Esteban-Fernandez, D.: Swot Mission Performance and Error Budget, in: IGARSS 2018 - 2018 IEEE International Geoscience and Remote Sensing Symposium, pp. 8625–8628, https://doi.org/10.1109/IGARSS.2018.8517385, 2018.

Peral, E., Esteban-Fernández, D., Rodríguez, E., McWatters, D., De Bleser, J.-W., Ahmed, R., Chen, A. C., Slimko, E., Somawardhana, R., Knarr, K., Johnson, M., Jaruwatanadilok, S., Chan, S., Wu, X., Clark, D., Peters, K., Chen, C. W., Mao, P., Khayatian, B., Chen, J., Hodges, R. E., Boussalis, D., Stiles, B., and Srinivasan, K.: KaRIn, the Ka-Band Radar Interferometer of the SWOT Mission: Design and in-Flight Performance, IEEE Transactions on Geoscience and Remote Sensing, 62, 1–27, https://doi.org/10.1109/TGRS.2024.3405343, 2024.

Schwatke, C., Dettmering, D., Bosch, W., and Seitz, F.: DAHITI – an innovative approach for estimating water level time series over inland waters using multi-mission satellite altimetry, Hydrology and Earth System Sciences, 19, 4345–4364, https://doi.org/10.5194/hess-19-4345-2015, 2015.

Sevdari, K. and Marmullaku, D.: Shapefile of European countries, DTU data, https://doi.org/10.11583/DTU.23686383.v1, 2023.

https://doi.org/10.5194/egusphere-2025-6366
Preprint. Discussion started: 11 February 2026

Simoes-Sousa, I. T., Camargo, C. M. L., Tavora, J., Piffer-Braga, A., Farrar, J. T., and Pavelsky, T. M.: The May 2024 Flood Disaster in Southern Brazil: Causes, Impacts, and SWOT-Based Volume Estimation, Geophysical Research Letters, 52, e2024GL112 442, https://doi.org/https://doi.org/10.1029/2024GL112442, e2024GL112442 2024GL112442, 2025.

SWOT: SWOT Level 2 Lake Single-Pass Vector Data Product, https://doi.org/10.5067/SWOT-LAKESP-2.0, 2024a.

SWOT: SWOT Level 2 Water Mask Pixel Cloud Data Product, https://doi.org/10.5067/SWOT-PIXC-2.0, 2024b.

SWOT: SWOT Level 2 River Single-Pass Vector Data Product, https://doi.org/10.5067/SWOT-RIVERSP-2.0, 2024c.

Taburet, N., Vayre, M., Calmettes, B., Zawadzki, L., Paris, A., Calmant, S., and Crétaux, J.: Copernicus Global Land Operations "Cryosphere and Water": Quality Assessment Report—Lake and River Water Level, https://land.copernicus.eu/en/technical-library/algorithm-theoretical-basis-document-near-real-time-water-level-lakes-and-rivers-v2.0/@@download/file, 2020.

Walter, K. M., Smith, L. C., and Stuart Chapin, F.: Methane bubbling from northern lakes: present and future contributions to the global methane budget, Philosophical Transactions of the Royal Society A: Mathematical, Physical and Engineering Sciences, 365, 1657–1676, https://doi.org/10.1098/rsta.2007.2036, 2007.

Wang, J., Pottier, C., Cazals, C., Battude, M., Sheng, Y., Song, C., Sikder, M. S., Yang, X., Ke, L., Gosset, M., et al.: The Surface Water and Ocean Topography Mission (SWOT) Prior Lake Database (PLD): Lake mask and operational auxiliaries, Authorea Preprints, https://doi.org/10.22541/au.170258987.72387777/v1, 2023.

Wigneron, J.-P., RIAZANOFF, S., Papa, F., BOURREL, L., Baghdadi, N., Frappart, F., and Normandin, C.: First results of the surface water ocean topography (SWOT) observations to rivers elevation profiles in the Cuvette Centrale of the Congo Basin, Frontiers in Remote Sensing, 5, https://doi.org/10.3389/frsen.2024.1466695, 2024.

Woolway, R. I., Kraemer, B. M., Lenters, J. D., Merchant, C. J., O'Reilly, C. M., and Sharma, S.: Global lake responses to climate change, Nature Reviews Earth & Environment, 1, 388–403, https://doi.org/https://doi.org/10.1038/s43017-020-0067-5, 2020.

WSP: Vandportalen, https://vandportalen.dk/, accessed: 31.07.2024, 2024.

Yu, L., Zhang, H., Gong, W., and Ma, X.: Validation of Mainland Water Level Elevation Products From SWOT Satellite, IEEE Journal of Selected Topics in Applied Earth Observations and Remote Sensing, 17, 13 494–13 505, https://doi.org/10.1109/JSTARS.2024.3435363, 2024.